On the Synoptic-Scale Lagrangian Autocorrelation Function

WESSAM Z. DAOUD,* JONATHAN D. W. KAHL, AND JUGAL K. GHORAI

Department of Mathematical Sciences, University of Wisconsin—Milwaukee, Milwaukee, Wisconsin

(Manuscript received 20 August 2001, in final form 15 September 2002)

ABSTRACT

A large set of 10-day, quasi-two-dimensional atmospheric trajectory model data is used to compute Lagrangian autocorrelation functions for horizontal velocity components and to determine their integral timescale T_L. The objectives of the study are to investigate the seasonal, interannual, and altitudinal behavior of T_L and to present the Lagrangian autocorrelation functions corresponding to synoptic-scale flow. Results indicate that the integral timescale T_L ranges from 15 to 24 h, with values for the meridional velocity component that are 10%–25% less than values for the zonal velocity component. The Lagrangian autocorrelation functions are modeled using Gaussian and second-order autoregressive autocorrelation models. The model fits to the observed autocorrelation functions were found to be of similar form to those determined for a 1-yr set of three-dimensional trajectory data, suggesting that these functions are robust with respect to synoptic-scale, tropospheric flow.

1. Introduction

One important component of air pollution modeling is the determination of particle spread in the vertical and horizontal directions downwind from a pollution source. This spread is often expressed as σ_y and σ_z, the standard deviations of particle position in the lateral (crosswind) and vertical directions, respectively.

The growth of particle plumes depends on the Lagrangian autocorrelation function. This function is the correlation, in the time domain, of successive velocities along the path and throughout the duration of particle travel. The Lagrangian timescale T_L is the integral of this autocorrelation function (Gifford 1987):

$$T_L = \int_0^\infty R_L(t)\, dt. \tag{1}$$

The Lagrangian timescale represents the time over which the velocity of a particle is self-correlated. It is roughly the time over which a particle maintains its initial velocity before experiencing a turbulent ''collision'' (Venkatram 1988). The autocorrelation function $R_L(t)$ in Eq. (1) is initially unity and approaches zero at long travel times (Draxler 1976). This function may therefore be interpreted as the extent to which a particle ''remembers'' its velocity between time zero and time t.

Taylor's (1921) theory of diffusion is the broad theoretical framework used to model σ_y, the standard deviation of particle spread:

$$\sigma_y^2 = 2\sigma_v^2 \int_0^T \int_0^t R_L(t)\, dt\, dT. \tag{2}$$

Here σ_v is the standard deviation of the lateral velocity fluctuations and T is the travel time. Equation (2), known as Taylor's theorem, states that the variance of particle position can be expressed in terms of a Lagrangian autocorrelation function and the variance of turbulent fluid velocities. The turbulence is assumed to be stationary and homogeneous (Arya 1999); thus Taylor's theorem is strictly valid only for small scales, that is, short travel times and/or small displacements.

In recent decades, analyses of short-range Lagrangian velocity fluctuations have led to improvements in short-range diffusion models. A statistical characterization of the synoptic-scale wind field may similarly provide information relevant to the study of long-range diffusion.

In this study we extend the application of one aspect of Taylor's theorem to longer timescales. Using a large database of modeled, 10-day atmospheric trajectories, we compute Lagrangian autocorrelation functions for horizontal velocity components and determine their integral timescale T_L. The objectives of the study are to investigate the seasonal, interannual, and altitudinal behavior of T_L and to present the Lagrangian autocorrelation functions corresponding to synoptic-scale flow. Other aspects of Taylor's theorem, including the velocity variance and dispersion, are not addressed in this work.

* Current affiliation: Montgomery Watson Harza Americas, Inc., Milwaukee, Wisconsin.

Corresponding author address: Jonathan D. W. Kahl, Atmospheric Science Group, Dept. of Mathematical Sciences, University of Wisconsin—Milwaukee, P.O. Box 413, Milwaukee, WI 53201.
E-mail: kahl@uwm.edu

2. Data and analysis method

The Lagrangian autocorrelation function was computed using a large database that contains 24 138 modeled atmospheric trajectories (National Snow and Ice Data Center 1997). Ten-day trajectories at two pressure altitudes, 500 and 700 hPa, were calculated to arrive daily (0000 UTC) at Summit, Greenland (72°34′N, 37°38′W; 3240 m MSL) during the period of 1946–89. The trajectory calculation procedure (Kahl et al. 1997) utilizes the geostrophic relationship to calculate horizontal wind components from gridded geopotential height data (Mass et al. 1987). Meteorological data for the calculation of 500- and 700-hPa trajectories were available from 1946 to 1989 (with the exception of 1956–57) and from 1962 to 1989, respectively. Each trajectory describes an air parcel's position, in latitude and longitude coordinates, at 1-h intervals throughout its 10-day transit to Summit. The resulting Lagrangian advection is quasi-two-dimensional in that a small, implied vertical motion is provided by the slope of the geopotential height surfaces. The trajectory data therefore represent a blending of model and observations, in that the trajectory model is based on observed meteorological fields.

The trajectory database was first partitioned by pressure altitude, season (winter = December–February; spring = March–May, etc.) and year. Next, the position data were decomposed into successive zonal and meridional (u and v) velocity components. The velocity components were then statistically evaluated to determine the Lagrangian velocity autocorrelation R_L for lags ξ up to 120 h (Stull 1988):

$$R_L(\xi) = \frac{\sum_{i=1}^{N-j} [(u_i - \overline{u}_i)(u_{i+j} - \overline{u}_{i+j})]}{\left[\sum_{i=1}^{N-j} (u_i - \overline{u}_i)^2\right]^{1/2}\left[\sum_{i=1}^{N-j} (u_{i+j} - \overline{u}_{i+j})^2\right]^{1/2}}, \quad (3)$$

where the two mean quantities refer to different portions of the trajectory under consideration: $\overline{u}_i = 1/(N - j)\ \Sigma_{i=1}^{N-j} u_i$ and $\overline{u}_{i+j} = 1/(N - J)\ \Sigma_{i=1}^{N-j} u_{i+j}$. Here u_i is the zonal velocity component, $N = 240$ is the number of 1-h velocity components in the trajectory, and $\xi = j\Delta t$ is the time lag. Similar expressions were used for the autocorrelation functions corresponding to the meridional velocity component, as well as for the scalar wind speed. Figure 1 shows example autocorrelation functions for one particular trajectory.

Using observed autocorrelation functions such as those shown in Fig. 1b, it is possible to use Eq. (1) to obtain the Lagrangian integral timescale T_L. However, because the autocorrelation functions are sometimes negative at large lags, calculating this parameter may be dependent upon oscillations of the autocorrelation function about zero. Thus, for the purpose of estimating the integral, we define the parameter B_0 as the time lag for which the autocorrelation function first reaches zero. The Lagrangian timescale is then obtained using

$$T_L = \int_0^{B_0} R_L(t)\, dt, \quad (4)$$

with integration carried out using an iterative trapezoidal rule (Press et al. 1986).

3. Results and discussion

a. Lagrangian timescale

To illustrate the characteristics of synoptic-scale Lagrangian autocorrelation functions and their integral timescale, we present a sample calculation corresponding to a single wintertime, 700-hPa trajectory (Fig. 1a). This particular trajectory originates in the Greenland Sea, follows southerly winds into the Arctic basin, stalls for a few days near the North Pole, then follows a rapid cyclonic path into the Greenland interior. After decomposing successive pairs of latitude and longitude coordinates into zonal, meridional, and scalar wind speeds, the autocorrelation functions were determined using Eq. (3). As shown in Fig. 1b, the autocorrelation functions for the individual velocity components decrease rapidly for lags up to about 1 day, become negative, reach a first (negative) minimum at lags between 1 and 2 days, and then reach a secondary maximum at lags of about 2 days. The autocorrelation function for the scalar wind speed decreases more steadily and exhibits less oscillatory behavior. The lags for which the functions first become zero (B_0) are 20, 57, and 49 h for the u, v, and scalar speed components, respectively. Applying these B_0 values to Eq. (4) yields Lagrangian integral timescales T_L of 11, 18, and 22 h for the u, v, and scalar speed components.

The wavelike behavior of the u and v autocorrelation functions is due to the response of an air parcel, during the course of its 10-day trajectory, to a wide range of correlated velocities provided by synoptic-scale eddies. In many trajectories the oscillatory behavior is more pronounced for the meridional component, reflecting alternating, multiday northward and southward advection, although this does not occur in the example shown in Fig. 1.

After computing B_0 and T_L for each of the 24 138 trajectories in the database, the results were aggregated by pressure and by season. The average values for each season are presented in Table 1. In general, Lagrangian integral timescales range from 15 to 24 h. Timescales for the v component are 10%–25% less than the corresponding u values, reflecting the increased variability in the meridional component of the northern hemispheric mid- and high-latitude flow, as compared with the zonal component. The T_L values tend to be slightly higher in the summer, although overall the seasonal variability is small. The timescale for wind speed is slightly

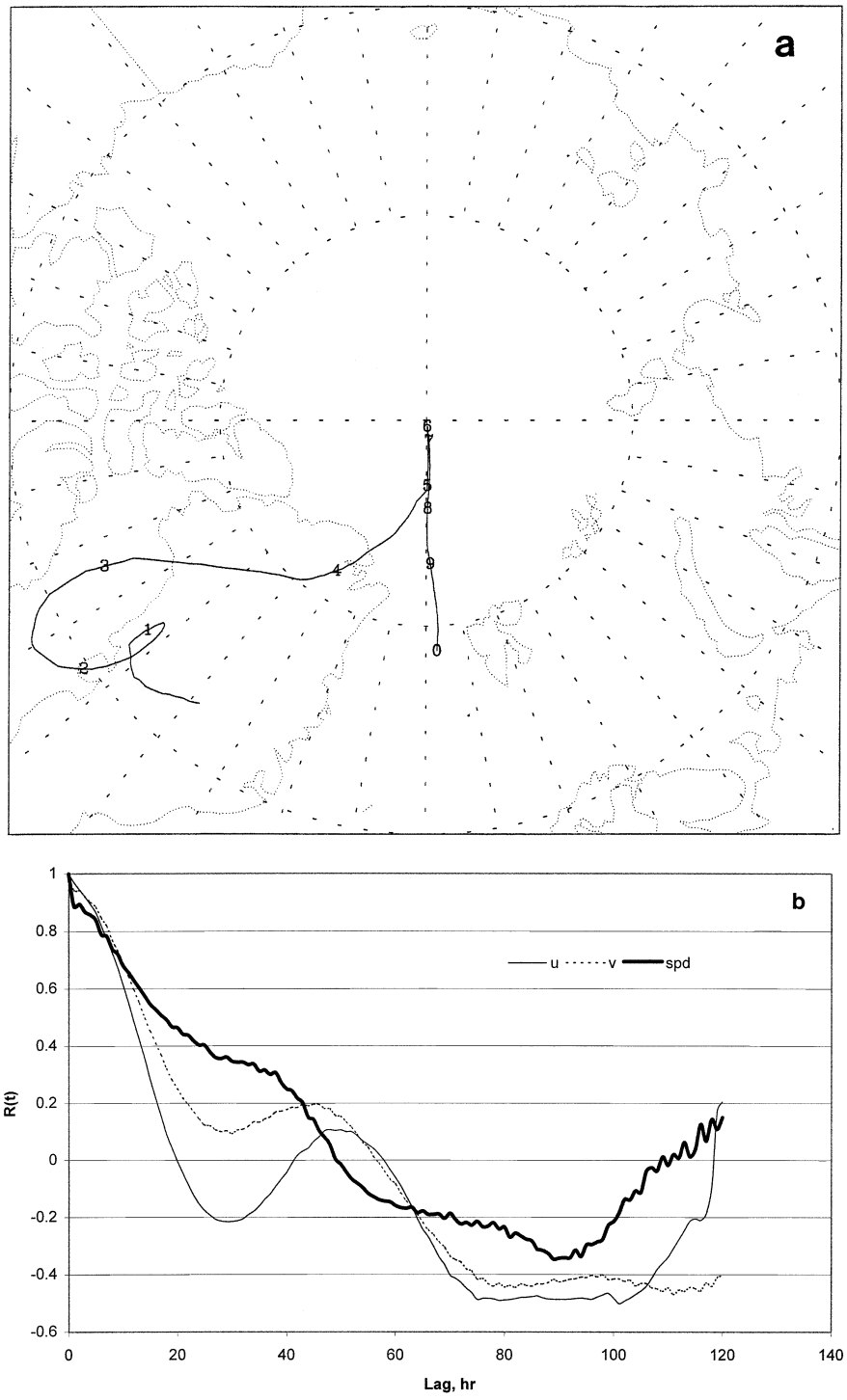

FIG. 1. (a) A sample wintertime, 700-hPa trajectory depicting the 10-day pathway of an air parcel enroute to Summit, Greenland. The symbols indicate the number of days upwind of Summit. (b) Lagrangian autocorrelation functions for the horizontal velocity components (u and v) and the scalar wind speed corresponding to the trajectory shown above.

TABLE 1. Mean Lagrangian timescales for zonal and meridional wind components and scalar wind speed at 500- and 700-hPa altitudes for all seasons.

		T_L (h)			B_0 (h)		
	Season	Zonal	Meridional	Speed	Zonal	Meridional	Speed
500 hPa	Autumn	20.8	15.4	22.8	42.6	42.6	48.4
	Winter	20.5	15.5	22.1	41.8	41.8	46.7
	Spring	20.0	15.6	21.4	41.2	41.2	45.7
	Summer	21.5	17.2	22.5	43.6	43.6	48.5
700 hPa	Autumn	22.7	20.9	23.3	45.6	45.6	50.1
	Winter	22.8	20.8	23.1	45.1	45.1	48.7
	Spring	22.3	20.4	23.4	43.9	43.9	49.8
	Summer	23.9	21.5	24.1	47.0	47.0	51.5

larger than that for the zonal component, ranging from 20 to 24 h.

The B_0 values in Table 1 range from 40 to 50 h. This means that, for 10-day transport as depicted by the 500- and 700-hPa isobaric trajectories, a Lagrangian air parcel's velocity at any time t is completely uncorrelated with its earlier or later velocity outside the time span $t \pm \sim 2$ days. Moreover, the T_L results suggest that an air parcel transported by synoptic-scale eddies maintains its ''identity,'' at least in terms of momentum, for no longer than 1 day.

Because the Lagrangian timescale represents an integration of winds throughout a 10-day trajectory, changes in the seasonally averaged timescale could reflect changes in the large-scale atmospheric circulation. Figure 2 shows a time series of T_L for zonal and meridional wind components corresponding to autumn-season, 500-hPa trajectories. Although substantial anomalies sometimes occur, particularly in the zonal values for 1957–65, we found no significant trend in T_L values for autumn or other seasons (not shown) over the study period.

The absence of any evidence of significant changes in atmospheric circulation features in our T_L time series analysis, such as the modes of the North Atlantic Oscillation (Rogers 1984), may be due to the details of the data and method. The trajectory database analyzed here is isobaric, whereas actual atmospheric motions are three-dimensional. A similar, multidecadal analysis of three-dimensional Lagrangian transport data may be more revealing in this regard. In addition, the global data assimilation model that produced the gridded meteorological data used in the trajectory calculations has undergone several major changes over the years (Trenberth and Olson 1988). A similar analysis using a ''frozen'' data assimilation model, such as those used in recent reanalysis efforts (e.g., Kalnay et al. 1996; Kistler et al. 2001), may yield results that are free of model-formulation artifacts.

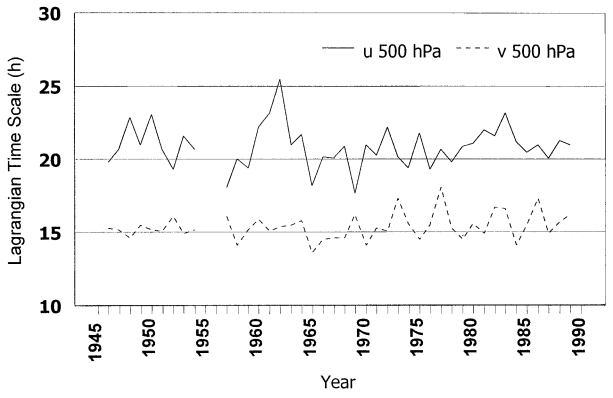

FIG. 2. Time series of mean Lagrangian timescales during the autumn season. Each seasonal value represents an average T_L for approximately 90 individual trajectories. Standard deviations (not shown) of seasonal mean values range from 10 to 15 h.

b. Lagrangian autocorrelation function

The Lagrangian autocorrelation function is difficult to measure directly. For turbulent flows with 0 means and Gaussian perturbations, an exponential form is often used (e.g., Panofsky and Dutton 1984). Theoretical expressions have been developed that correspond to homogeneous and isotropic turbulent flow for engineering applications (e.g., Yeung and Pope 1989; Nakao 1997), but these forms are not relevant for synoptic-scale atmospheric motions. Our analysis, which includes the determination of autocorrelation functions that correspond to a large number of modeled, 10-day trajectories, gives us the opportunity to determine its general form.

An example, ensemble mean autocorrelation function corresponding to the autumn-season, 500-hPa meridional wind component is shown in Fig. 3. The error bars are drawn at $\pm$ one standard deviation from the mean value of $R_L(t)$. The standard deviation of the seasonal mean autocorrelation values is seen to rise substantially at increasing lags, reflecting an increasing degree of synoptic-scale variability in wind flow.

Figure 3 includes experimental fits to this function. An exponential form provides a poor fit to the observed autocorrelation data. A Gaussian model of the form

$$R_L(t) = a \exp\left[\frac{-(t - b)^2}{2c^2}\right], \qquad (5)$$

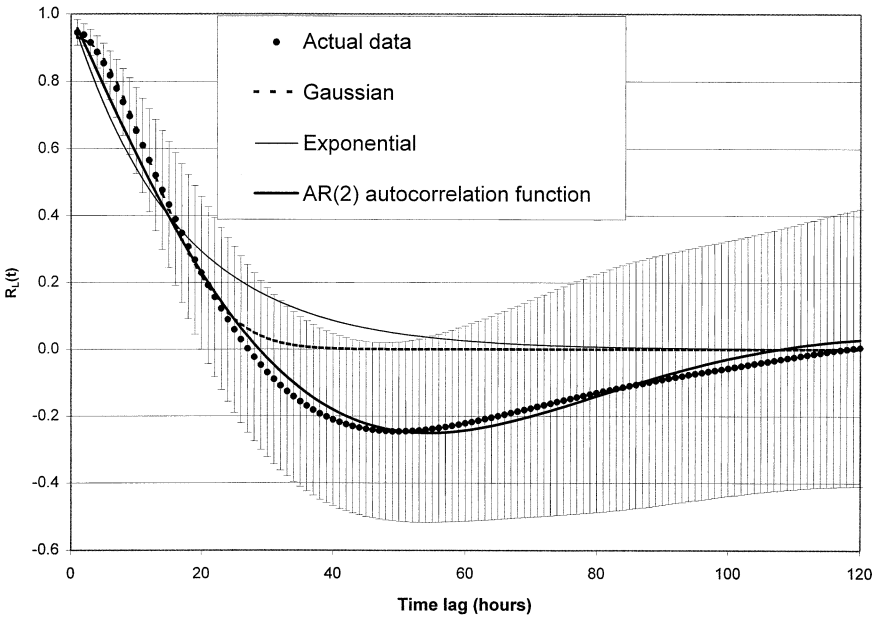

FIG. 3. Observed (with ± one std dev error bars) and modeled Lagrangian autocorrelation functions for the autumn-season, 500-hPa meridional wind component. The AR(2) autocorrelation model fits the entire function well; the Gaussian model fits the function better in the range 1 h $\leq t \leq B_0$ (where t is the time lag). The exponential curve does not provide a good fit to the observed autocorrelation data.

fits the data well over the range 1 h $\leq t \leq B_0$, where B_0 is the lag for which the autocorrelation function first reaches 0. An autocorrelation function corresponding to a second-order autoregressive [AR(2)] model (Shumway and Stoffer 2000), of the form

$$R_L(t) = \frac{\cos(at + b)}{c^t \cos b}, \tag{6}$$

provides a good fit over the entire range of lags, 1 h $\leq t \leq 120$ h.

Although the AR(2) autocorrelation model [Eq. (6)] provides a good fit ($r^2 = 0.996$, where r is correlation coefficient) to the function over the entire range of lags, the Gaussian model [Eq. (5)] fits the function better in the region prior to the first zero crossing where $t = B_0$ (in the 1 h $\leq t \leq B_0$ region, the Gaussian model has a squared correlation coefficient of $r^2 > 0.998$). Both models display the proper asymptotic behavior at large lag times, that is, $R_L \to 0$ as $t \to \infty$.

The coefficients for the Gaussian and AR(2) models [Eqs. (5) and (6)] shown in Fig. 3, as well as for autocorrelation functions corresponding to different altitudes, seasons, and wind velocity components, are shown in Table 2. It is clear that all functions are described well by AR(2) and Gaussian fits.

The autocorrelation functions described in Table 2 are similar for both 700- and 500-hPa Lagrangian airflow. In an attempt to determine whether any differences would be observed in autocorrelation functions corresponding to three-dimensional trajectories, we performed a similar analysis using 1 yr (1986) of three-dimensional trajectories. The trajectories were calculated using the hybrid isentropic/mixed-layer model developed by Harris and Kahl (1994). This model assumes isentropic transport; however, when air parcels reach altitudes within 100 m of the earth's surface, transport is modeled by an average wind of the 100–600-m AGL layer. This accounts for inconsistencies that might arise should the isentropic surface intersect the earth's surface.

As shown in Table 2, the autocorrelation functions determined for the three-dimensional trajectories are of similar form to those found for the quasi-two-dimensional 700- and 500-hPa trajectories. This suggests that the forms for the Lagrangian autocorrelation functions, as presented in Table 2, are generally applicable to synoptic-scale tropospheric flow.

4. Summary and conclusions

In this study, we have determined the Lagrangian autocorrelation function $R_L(t)$ and its integral timescale T_L, corresponding to synoptic-scale tropospheric flow. The autocorrelation functions typically exhibit an oscillatory behavior because of the response of air parcels to a wide range of correlated velocities provided by synoptic-scale eddies. The integral timescale T_L ranges from 15 to 24 h, with values for the meridional velocity component that are 10%–25% less than values for the zonal velocity component.

Time series of seasonally averaged Lagrangian timescales revealed considerable structure, but no overall

TABLE 2. AR(2) autocorrelation and Gaussian models of the Lagrangian autocorrelation function $R_L(t)$, where t is the lag (h), as a function of trajectory altitude, season, and velocity component. For the AR(2) model, the squared correlation coefficient (r^2) values show the quality of the fit for the entire function, 1 h $\leq t \leq$ 120 h. Squared correlation coefficient values for the Gaussian model correspond to the region 1 h $\leq t \leq B_0$, where B_0 is the lag for which the autocorrelation function first reaches 0.

			AR(2) autocorrelation model coefficients: $R_L(t) = \frac{\cos(at + b)}{c^t \cos b}$				Gaussian coefficients: $R_L(t) = a \exp\left[\frac{-(t-b)^2}{2c^2}\right]$			
Trajectory alt	Season	Velocity component	a	b	c	r^2	a	b	c	r^2 (1 h $\leq t \leq B_0$)
700 hPa	Winter	u	0.0296	0.3855	1.0205	0.9973	0.9751	−1.3606	15.8114	0.9992
		v	0.0303	0.4188	1.0215	0.9982	0.9394	−0.9330	15.0716	0.9992
		Speed	0.0222	0.5940	1.0214	0.9992	1.0017	−6.1175	19.1578	0.9995
	Spring	u	0.0302	0.3836	1.0203	0.9964	0.9626	−0.4741	15.2020	0.9990
		v	0.0316	0.3907	1.0211	0.9981	0.9209	−0.1675	14.7791	0.9990
		Speed	0.0211	0.6190	1.0211	0.9992	0.9742	−5.3374	19.1967	0.9994
	Summer	u	0.0291	−2.7986	1.0189	0.9982	0.9617	−1.4518	17.1443	0.9990
		v	0.0308	0.3608	1.0210	0.9987	0.8912	−0.0808	15.6836	0.9989
		Speed	0.0198	0.6339	1.0219	0.9992	0.9478	−5.9170	20.2943	0.9994
	Autumn	u	0.0300	0.3621	1.0207	0.9971	0.9634	−0.9747	15.8306	0.9989
		v	0.0314	0.3782	1.0218	0.9982	0.9137	−0.2442	14.9828	0.9989
		Speed	−0.0208	−0.6222	1.0216	0.9994	0.9927	−6.8641	20.0388	0.9995
500 hPa	Winter	u	0.0361	0.2828	1.0250	0.9971	0.9825	−1.3827	14.2206	0.9991
		v	0.0382	0.4632	1.0236	0.9962	0.9437	0.1547	11.5318	0.9981
		Speed	0.0312	0.3114	1.0239	0.9994	1.0218	−5.4032	17.8711	0.9991
	Spring	u	0.0350	3.4796	1.0268	0.9955	0.9765	−0.9577	13.4475	0.9992
		v	0.0367	0.4981	1.0235	0.9957	0.9385	0.3454	11.5122	0.9983
		Speed	0.0271	−5.7995	1.0235	0.9990	1.0192	−5.3265	17.3732	0.9993
	Summer	u	0.0300	−2.7314	1.0232	0.9959	0.9718	−1.2975	14.9954	0.9992
		v	0.0355	−2.6949	1.0226	0.9964	0.9240	0.4492	12.5074	0.9984
		Speed	0.0239	−2.6061	1.0224	0.9994	1.0315	−7.0701	19.3033	0.9993
	Autumn	u	0.0288	0.4816	1.0240	0.9955	0.9816	−1.5147	14.4958	0.9992
		v	0.0398	0.4279	1.0246	0.9950	0.9314	0.6098	11.3341	0.9978
		Speed	0.0265	−5.8446	1.0225	0.9992	1.0195	−5.8004	18.6348	0.9992
3D data		u	0.0317	−2.7829	1.0220	0.9949	0.9664	0.0808	14.2576	0.9992
		v	0.0365	50.5069	1.0249	0.9976	0.9403	−0.1295	13.9739	0.9994
		Speed	0.0260	−2.6707	1.0242	0.9978	1.0101	−4.9058	17.4292	0.9997

trend, over the period of 1946–89. We propose that the Lagrangian timescale may have some utility as a diagnostic indicator of large-scale circulation changes, but it may be necessary to perform a similar analysis using trajectories based on a frozen data assimilation system, such as those used in recent reanalysis efforts (e.g., Kistler et al. 2001).

Our results indicate that the Lagrangian autocorrelation function can be successfully modeled using Gaussian and AR(2) autocorrelation functions. The AR(2) autocorrelation model fits the functions well ($r^2 \geq 0.995$) over the entire range of lags examined; the Gaussian model fits the data well ($r^2 > 0.998$) for lags ranging from $t = 1$ h to $t = B_0$, the first zero crossing. The Gaussian and AR(2) autocorrelation models of the observed autocorrelation functions were found to be of similar form to those determined for a 1-yr set of three-dimensional trajectory data, suggesting that these functions are robust with respect to synoptic-scale, tropospheric flow.

Statistical characterizations of Lagrangian wind speed and turbulence observations have been made for small scales (e.g., Hanna 1979, 1981), leading to the development and refinement of many short-range diffusion models. It has long been known that horizontal dispersion aloft is due in large part more to synoptic-scale wind variability than to subsynoptic-scale turbulence (Bolin and Persson 1975; Pasquill and Smith 1983). Thus the properties of synoptic-scale winds, including their Lagrangian statistical behavior, can be used to infer long-range dispersion.

Several investigators have previously utilized synoptic-scale wind data to infer long-range diffusion (e.g., Durst et al. 1959; Heffter 1965; Samson 1980). However, a recent investigation by Walcek (2002) suggests that the selection of appropriate dispersion coefficients in Lagrangian models is highly problematic. The current paper presents an initial statistical characterization of Lagrangian wind observations on the synoptic scale, which thus have application to the improvement of long-range dispersion parameterizations (e.g., Maryon and Best 1995; Zannetti 1984; Nieuwstadt and van Dop 1982). Subsequent work in this area could involve, for example, the relationship between velocity variance and dispersion, aspects of Taylor's theorem that were not considered here.

The results presented here may also be used to evaluate uncertainties (i.e., quality and coherency) in ensemble dispersion models (Straume et al. 1998; Straume 2001; Hanna et al. 1998). For example, the Lagrangian statistics in this study may be used to constrain similar properties derived from trajectory ensembles produced by such models. In addition, our results have potential application to the problem of extending existing climatological dispersion models to longer distances (Goyal et al. 1994; Guldman and Kim 2001).

Acknowledgments. We thank the anonymous reviewers for their thoughtful comments.

REFERENCES

Arya, S. P., 1999: *Air Pollution Meteorology and Dispersion.* Oxford University Press, 310 pp.

Bolin, B., and C. Persson, 1975: Regional dispersion and deposition of atmospheric pollutants with particular application to sulfur pollution over Western Europe. *Tellus,* **27,** 281–310.

Draxler, R. R., 1976: Determination of atmospheric diffusion parameters. *Atmos. Environ.,* **10,** 99–105.

Durst, C. S., A. F. Crossley, and N. E. Davis, 1959: Horizontal diffusion in the atmosphere as determined by geostrophic trajectories. *J. Fluid Mech.,* **6,** 401–422.

Gifford, F. A., 1987: The time-scale of atmospheric diffusion considered in relation to the universal diffusion function, f_1. *Atmos. Environ.,* **21,** 1315–1320.

Goyal, P., M. P. Singh, and T. K. Bandyopadhyay, 1994: Environmental studies of SO_2, SPM and NO_x over Agra, with various methods of treating calms. *Atmos. Environ.,* **28,** 3113–3123.

Guldman, J. M., and H. Y. Kim, 2001: Modeling air quality in urban areas: A cell-based statistical approach. *Geogr. Anal.,* **33,** 156–180.

Hanna, S. R., 1979: Some statistics of Lagrangian and Eulerian wind fluctuations. *J. Appl. Meteor.,* **18,** 518–525.

——, 1981: Lagrangian and Eulerian time scale relations in the daytime boundary layer. *J. Appl. Meteor.,* **20,** 242–249.

——, J. C. Chang, and M. E. Fernau, 1998: Monte Carlo estimates of uncertainties in predictions by a photochemical grid model (UAM-IV) due to uncertainties in input variables. *Atmos. Environ.,* **32,** 3619–3628.

Harris, J. M., and J. D. W. Kahl, 1994: Analysis of 10-day isentropic flow patterns for Barrow, Alaska: 1985–1992. *J. Geophys. Res.,* **99,** 25 845–25 855.

Heffter, J. L., 1965: The variation of horizontal diffusion parameters with time for travel periods of one hour or longer. *J. Appl. Meteor.,* **4,** 153–156.

Kahl, J. D. W., D. A. Martinez, H. Kuhns, C. I. Davidson, J.-L. Jaffrezo, and J. M. Harris, 1997: Air mass trajectories to Summit, Greenland: A 44-year climatology and some episodic events. *J. Geophys. Res.,* **102,** 26 861–26 875.

Kalnay, E., and Coauthors, 1996: The NCEP/NCAR 40-Year Reanalysis Project. *Bull. Amer. Meteor. Soc.,* **77,** 437–471.

Kistler, R., and Coauthors, 2001: The NCEP–NCAR 50-Year Reanalysis: Monthly means CD-ROM and documentation. *Bull. Amer. Meteor. Soc.,* **82,** 247–268.

Maryon, R. H., and M. J. Best, 1995: Estimating the emissions from a nuclear accident using observations of radioactivity with dispersion model products. *Atmos. Environ.,* **29,** 1853–1869.

Mass, C. F., H. F. Edmon, H. J. Friedmon, N. R. Cheney, and E. E. Recker, 1987: The use of compact disks for the storage of large meteorological and oceanographic data sets. *Bull. Amer. Meteor. Soc.,* **68,** 1556–1558.

Nakao, H., 1997: Exact expression of Lagrangian velocity autocorrelation function in isotropic homogeneous turbulence. *Monte Carlo Meth. Appl.,* **3,** 225–240.

National Snow and Ice Data Center, 1997: *The Greenland Summit Ice Cores.* National Snow and Ice Data Center, University of Colorado, Boulder, and the World Data Center-A for Paleoclimatology, National Geophysical Data Center, Boulder, CO, CD-ROM.

Nieuwstadt, F. T., and H. van Dop, 1982: *Atmospheric Turbulence and Air Pollution Modeling.* D. Reidel, 358 pp.

Panofsky, H. A., and J. A. Dutton, 1984: *Atmospheric Turbulence.* John Wiley and Sons, 397 pp.

Pasquill, F., and F. B. Smith, 1983: *Atmospheric Diffusion.* Ellis Horwood, 437 pp.

Press, W. H., B. P. Flannery, S. A. Teukolsky, and W. T. Vetterling, 1986: *Numerical Recipes: The Art of Scientific Computing.* Cambridge University Press, 818 pp.

Rogers, J. C., 1984: The association between the North Atlantic Oscillation and the Southern Oscillation in the Northern Hemisphere. *Mon. Wea. Rev.,* **112,** 1999–2015.

Samson, P. J., 1980: Trajectory analysis of summertime sulfate concentrations in the northeastern United States. *J. Appl. Meteor.,* **19,** 1382–1394.

Shumway, R. H., and D. S. Stoffer, 2000: *Time Series Analysis and Its Applications.* Springer-Verlag, 549 pp.

Straume, A. G., 2001: A more extensive investigation of the use of ensemble forecasts for dispersion model evaluation. *J. Appl. Meteor.,* **40,** 425–445.

——, E. N. Koffi, and K. Nodop, 1998: Dispersion modeling using ensemble forecasts compared to ETEX measurements. *J. Appl. Meteor.,* **37,** 1444–1456.

Stull, R. B., 1988: *An Introduction to Boundary Layer Meteorology.* Kluwer Academic, 666 pp.

Taylor, G. I., 1921: Diffusion by continuous movements. *Proc. London Math. Soc.,* **20,** 196–211.

Trenberth, K. E., and J. G. Olson, 1988: An evaluation and intercomparison of global analyses from the National Meteorological Center and the European Centre for Medium Range Weather Forecasts. *Bull. Amer. Meteor. Soc.,* **69,** 1047–1056.

Venkatram, A., 1988: An interpretation of Taylor's statistical analysis of particle dispersion. *Atmos. Environ.,* **22,** 865–868.

Walcek, C. J., 2002: Effects of wind shear on pollution dispersion. *Atmos. Environ.,* **36,** 511–517.

Yeung, P. K., and S. B. Pope, 1989: Lagrangian statistics from direct numerical simulation of isotropic turbulence. *J. Fluid Mech.,* **207,** 531–544.

Zannetti, P., 1984: New Monte Carlo scheme for simulating Lagrangian particle diffusion with wind shear effects. *Appl. Math. Modell.,* **8,** 188–192.